Available online at www.sciencedirect.com

SCIENCE DIRECT

Developmental Biology 280 (2005) 344–361

DEVELOPMENTAL BIOLOGY

www.elsevier.com/locate/ydbio

Sox9 neural crest determinant gene controls patterning and closure of the posterior frontal cranial suture

David E. Sahar, Michael T. Longaker*, Natalina Quarto*

Department of Surgery, The Children's Surgical Research Program, Stanford University School of Medicine, 257 Campus Drive Meyer Building, Stanford University, Stanford, CA 94305-5148, USA

Received for publication 8 July 2004, revised 19 January 2005, accepted 19 January 2005

Abstract

Cranial suture development involves a complex interaction of genes and tissues derived from neural crest cells (NCC) and paraxial mesoderm. In mice, the posterior frontal (PF) suture closes during the first month of life while other sutures remain patent throughout the life of the animal. Given the unique NCC origin of PF suture complex (analogous to metopic suture in humans), we performed quantitative real-time PCR and immunohistochemistry to study the expression pattern of the NCC determinant gene *Sox9* and select markers of extracellular matrix. Our results indicated a unique up-regulated expression of *Sox9*, a regulator of chondrogenesis, during initiation of PF suture closure, along with the expression of specific cartilage markers (*Type II Collagen* and *Type X Collagen*), as well as cartilage tissue formation in the PF suture. This process was followed by expression of bone markers (*Type I Collagen* and *Osteocalcin*), suggesting endochondral ossification. Moreover, we studied the effect of haploinsufficiency of the NCC determinant gene *Sox9* in the NCC derived PF suture complex. A decrease in dosage of *Sox9* by haploinsufficiency in NCC-derived tissues resulted in delayed PF suture closure. These results demonstrate a unique development of the PF suture complex and the role of *Sox9* as an important contributor to timely and proper closure of the PF suture through endochondral ossification.

Keywords: Neural crest cells; *Sox9*; Chondrogenesis; Endochondral ossification; Cranial suture patterning; Posterior frontal suture

Introduction

Calvaria origin can be traced back to the neural crest and paraxial mesoderm. The frontal bone plates and the PF suture (analogous to metopic suture in humans) originate from NCC in vertebrates (Couly et al., 1993; Jiang et al., 2002; Le Lievre, 1978; Morriss-Kay, 2001; Noden, 1975). Normal craniofacial development is dependent on precise tissue contributions by the NCC and paraxial mesoderm and controlled gene regulation of sutures positioned between the calvarial growth fronts.

Aberration at any control level could potentially lead to premature suture closure (craniosynostosis) or delayed suture closure (Opperman, 2000; Rice et al., 2003; Wilkie, 1997). Since the first report of a genetic link to craniosynostosis in 1993 (Jabs et al., 1993), heterozygous mutations in at least 6 different genes have been associated with this condition; fibroblast growth factor receptors (*FGFRs*), Transcription factors *MSX2* and *TWIST*, and *Fibrillin-1* (Bellus et al., 1996; Howard et al., 1997; Meyers et al., 1996; Muenke et al., 1994; Sood et al., 1996). Expression and interaction of *Fgfrs*, *Msx2*, and *Twist* genes have been described extensively in murine cranial sutures (Ignelzi et al., 2003; Iseki et al., 1997, Ishii et al., 2003; Rice et al., 2003; Warren et al., 2003). However, sporadic cases of craniosynostosis, without an identified gene mutation, constitute the majority of children with craniosynostosis (Gorlin et al., 1990; Wilkie and Morriss-Kay, 2001). The sporadic cases suggest a larger repertoire of genes involved in normal suture development.

The PF suture is the only suture whose mesenchyme and flanking calvarial bone plates are derived from NCC. Since this is the only cranial suture that closes during the lifetime of

* Corresponding authors. Fax: +1 650 736 1705.
E-mail addresses: Longaker@stanford.edu (M.T. Longaker), quarto@unina.it (N. Quarto).

0012-1606/$ - see front matter © 2005 Elsevier Inc. All rights reserved.
doi:10.1016/j.ydbio.2005.01.022

mice, it warrants the question of whether the unique origin of this suture complex is responsible for its distinctive fate. To date, no analytical study of PF suture development in mice has been reported. Since, the closing PF suture complex in mice is of neural crest origin, NCC determinant genes may contribute to its unique fate.

Sox9, a transcription factor and a member of group E sox genes, is a NCC determinant gene as well as a direct regulator of chondrogenesis (Akiyama et al., 2002; Bi et al., 2001; Cheung and Briscoe, 2003; de Crombrugghe et al., 2000; Mori-Akiyama et al., 2003; Spokony et al., 2002). Heterozygous mutations in *SOX9* in humans lead to campomelic dysplasia (CD), a severe dwarfism syndrome characterized by anomalies of endochondral skeleton elements (Foster et al., 1994; Wagner et al., 1994). Heterozygous mutation of *Sox9* in mice causes craniofacial anomalies resembling CD patients (Bi et al., 2001). *Slug*, a zinc-finger transcription factor and a member of the Snail family, is expressed in migratory NCC (Jiang et al., 1998; Nieto et al., 1994). To date, there has been no study examining NCC markers *Sox9* or *Slug* and their downstream targets in closing and patent sutures.

In mice and rats, the PF suture closes during the first month of life, while the sagittal (SAG) and coronal (COR) sutures remain patent throughout the life of the animal (Bradley et al., 1996; Moss, 1958; Opperman, 2000). The divergent suture fate, along with availability of transgenic lines in mice, makes this model ideal for studying suture development and biology. The temporal sequence of suture mesenchyme ossification and its genomic expression pattern is not well characterized in mice. In this study, we have analyzed histologically and morphologically the temporal sequence of events during the first month of life in PF suture complex. Moreover, we have investigated the expression of NCC markers *Sox9* and its target genes, as well as *Slug* in the NCC derived PF suture. Finally we have analyzed the PF suture complex in mice that are *Sox9* conditionally haploinsufficient in NCC derived tissues.

Materials and methods

Animals and generation of mutant mice

The animals were cared for in accordance with the Institutional Animal Care and the Use Committee at Stanford University. $Sox9^{flox/WT}$ carrying mice were a generous gift from Marie-Christine Chaboissier and Andreas Schedl (INSERM U470, Centre de Biochimie, Nice, France) (Akiyama et al., 2002). *Wnt1-Cre* mice were obtained from Jackson Laboratories (Bar Harbor, ME). CD-1 mice were obtained from Charles River Laboratories (Wilmington, MA). All animals were kept in a temperature and moisture-controlled animal facility. CD-1 animals were sacrificed on the exact day post-natal (p) based on birth date (day 0). Time points included: p1, p3, p5, p6, p7, p8, p9, p10, p11, p12, p13, p14, p15, p16, p17, p25. *Sox9* haploinsufficient mice in NCC derived tissues were obtained by crossing mice homozygous for *Wnt1-Cre*, constitutively expressing *Cre*, with mice heterozygotic for *Sox9* floxed alleles ($Sox9^{flox/WT}$). All newborns were genotyped by PCR using DNA from skin. Target genotype in offspring followed mendelian inheritance pattern. The following primers were used for detecting target genotypes: *Cre*, (F:TCCAATTTACTGACCGTACACCAA; R: CCTGATCCTGGCAATTTCGGCTA); $Sox9^{flox}$, (F: GTCAAGCGACCCATGAACGC; R: TGGTAATGAGTCATACACAGTAC).

Tissue harvest

Mice were sacrificed by CO_2 asphyxiation and the calvariae were dissected. PF and SAG sutures were meticulously harvested from CD-1 mice using Surgical Acuity™ loupes. Measurements were taken of the PF and SAG sutures immediately after harvest using a caliper and a ruler. After clearly identifying the lambdoidal, SAG, COR, PF and anterior frontal (AF) sutures, the PF and SAG suture complexes inclusive of the suture mesenchyme, adjacent osteogenic fronts of the opposing calvarial growth plates, and the underlying dura mater were carefully dissected, separated, and harvested using fine, slightly curved sharp tip scissors (finescience.com). Suture width after harvest measured 0.6–0.8 mm. Suture length varied with animal age. The bregma was excluded.

Tissue RNA extraction

1 litter (on average 8 animals) of mice was used for each time point. Pooled sutures from each litter were homogenized in 0.6 ml of Trizol (Invitrogen, Carlsbad, CA) using a Pellet Pestle Motor, (Kontes) according to manufacturer's protocol. RNA was extracted and precipitated using chloroform and 2-propanol. RNA was further washed with DEPC treated 70% ethanol. RNA was isolated from three independent litters of mice.

Tissue processing and staining

Following sacrifice of animals described above, the calvariae of animals were harvested and immediately fixed in fresh, chilled 4% paraformaldehyde overnight at 4°C followed by 24 to 48 h of decalcification in Formical-2000 (Decal Chemical Company, Congers, NY). Each calvaria was divided coronally through the bregma to separate the PF from the SAG sutures. The specimens then underwent dehydration in a graded ethanol series and were paraffin embedded. The entire blocks were serially sectioned (5–7 μm) totaling approximately 400 sections for each block. Every other slide was stained with hematoxylin and eosin (H&E) for evaluation and the selected slides were used for immunohistochemistry and Safranin-O. H&E and Safranin-O staining were performed according to standard procedures. The stained sutures

were examined with Carl Zeiss Axioplan 2 (Zeiss, Thornwood, NY) microscope from 10× to 100× magnification. Images were captured by AxioVision (Zeiss, Thornwood, NY) and combined by Adobe Photoshop (Adobe Systems, San Jose, CA). Closure was defined as mature bony bridge between the osteogenic fronts.

Morphometric analysis

For gross morphometric analysis, fixed whole calvariae were stained overnight in 0.1% Alizarin red and/or Alcian blue according to standard procedures, followed by clearing with 50% Glycerol for 2–4 weeks. Measurements were made in triplicate per time point using a caliper and a ruler. Skull length was measured from the anterior margin of frontal bone to the posterior margin of occipital bone. Skull width was defined as the maximum length between the lateral aspect of parietal bones as seen from top view. The PF suture measurement was made from jugum limitans (landmark between PF and AF sutures) to bregma (confluence of SAG, COR and PF sutures). The SAG suture was measured from the bregma to the lambdoidal suture.

Quantitative real-time PCR

Purified and quantified RNA were treated with DNAse I (Ambion, Austin, TX) to clear genomic DNA. 5 μg of total RNA from each time point was reverse transcribed to cDNA using random primer hexamers (Invitrogen, Carlsbad, CA). For quantitative real-time PCR, primers were designed with Primer Express™ software (Applied Biosystems). Each primer was subjected to PCR to ensure single primary amplicon as evidenced by 2% agarose gel electrophoresis to be <200 bp for maximum efficiency. SYBR® Green PCR Master Mix (Applied Biosystems) was used for fluorescence. Primer sequences used: *Sox9*, (*F*: ACGGCTCCAGCAAGAACAAG; *R*: TTGTGCAGATGCGGGTACTG); *Slug*, (*F*: CCATCGAAGCTGAGAAGTTTCA; *R*: CCCAGGCTCACATATTCCTTGT); *Type I Collagen* (*F*: AACCCGAGGTATGCTTGATCT; *R*: CCAGTTCTTCATTGCATTGC); *Type II Collagen* (*F*: CGAGTGGAAGAGCGGAGACTAC; *R*: CCAGTTTTTCCGAGGGACAGT); *Type X Collagen* (*F*: TGCTGCCTCAAATACCCTTTCT; *R*: TGGCGTATGGGATGAAGTATTG); *Fgf-2* (*F*: GTCACGGAAATACTCCAGTTGGT; *R*: CCCGTTTTGGATCCGAGTTT); *Fgf-18* (*F*: CAAGTCCTGGGCCGTAGGA; *R*: GCCCTTGATCCGGACTTGA); *Osteocalcin* (*F*: GGGAGACAACAGGGAGGAAAC; *R*: CAGGCTTCCTGCCAGTACCTT). Samples along with primers and Syber Green Master Mix (Applied Biosystems, Foster City, CA) were loaded in 384 well sealed plates and the reaction was run in an ABI Prism 7900 HT (Applied Biosystems) according to the manufacturer's protocol. *Gapdh* (Applied Biosystems) was used for internal control.

Standard curve method of quantitation was used to calculate expression of target genes relative to the housekeeping gene *Gapdh*. Four serial dilutions of cDNA (1:4) were made for the calibration curve and trend lines were drawn using Ct values versus log of dilutions for each target gene and *Gapdh* run in triplicate with correlation coefficient ($R^2 > 0.99$). Relative expressions were calculated using line equations derived from calibration curves and obtaining ratios of target gene to *Gapdh* for each time point. For each gene, experiments were run at least three times using three independent litters of mice. The error bars reflect variability between litters.

Immunohistochemistry

Selected paraffin embedded sections were chosen, deparaffinized, rehydrated and antigen retrieval was performed. For extracellular matrix antigens, sections were treated with pepsin (Sigma, St. Louis, MO) for 1 h at 37°C. The Vectastain ABC system (Vector Laboratories, Burlingame, CA) was used according to the manufacturer's protocol for immunoperoxidase detection of targeted antigen. Primary antibodies against Sox9, Slug and Type II Collagen (Santa Cruz Biotechnology, Inc., Santa Cruz, CA), Osteocalcin (Biomedical Technologies Inc., Stoughton, MA) and Type X Collagen (Quartett Immunodiagnostika and Biotechnologie, Berlin, Germany) were used in serial dilutions (1:50, 1:100, 1:200). Appropriate biotinylated secondary antibodies (Vector Laboratories, Burlingame, CA) were used in 1:500 dilutions. Non-specific serum of primary antibody host species was used as negative control.

Results

PF and SAG suture characteristics during the first month of life

Current understanding of suture biology suggests involvement of all three suture complex components in suture closure; osteogenic fronts, suture mesenchyme, and the underlying dura mater (Greenwald et al., 2001; Opperman et al., 1993; Roth et al., 1996). As such, all three components above will form our experimental model. This complex lies between bregma posteriorly and jugum limitans anteriorly (Figs. 1A and B). To study physical characteristics of the PF and SAG sutures during development in mice, we performed morphometric analysis on Alizarin red/Alcian blue stained calvariae during the first month of life in timed birth mice. Morphometric analysis demonstrated that calvaria length and width growth is greatest during the first 2 weeks of life, however, the calvaria continues to grow thereafter at a slower pace during third and fourth week of life (Fig. 1C). Calvaria length increases from 8.5 to 14 mm while calvarial width increases from 7 to slightly over 11 mm from birth to 25 days of age. To determine the intrinsic growth of the PF and SAG sutures we measured the length of suture itself, based on well-known anatomical landmarks

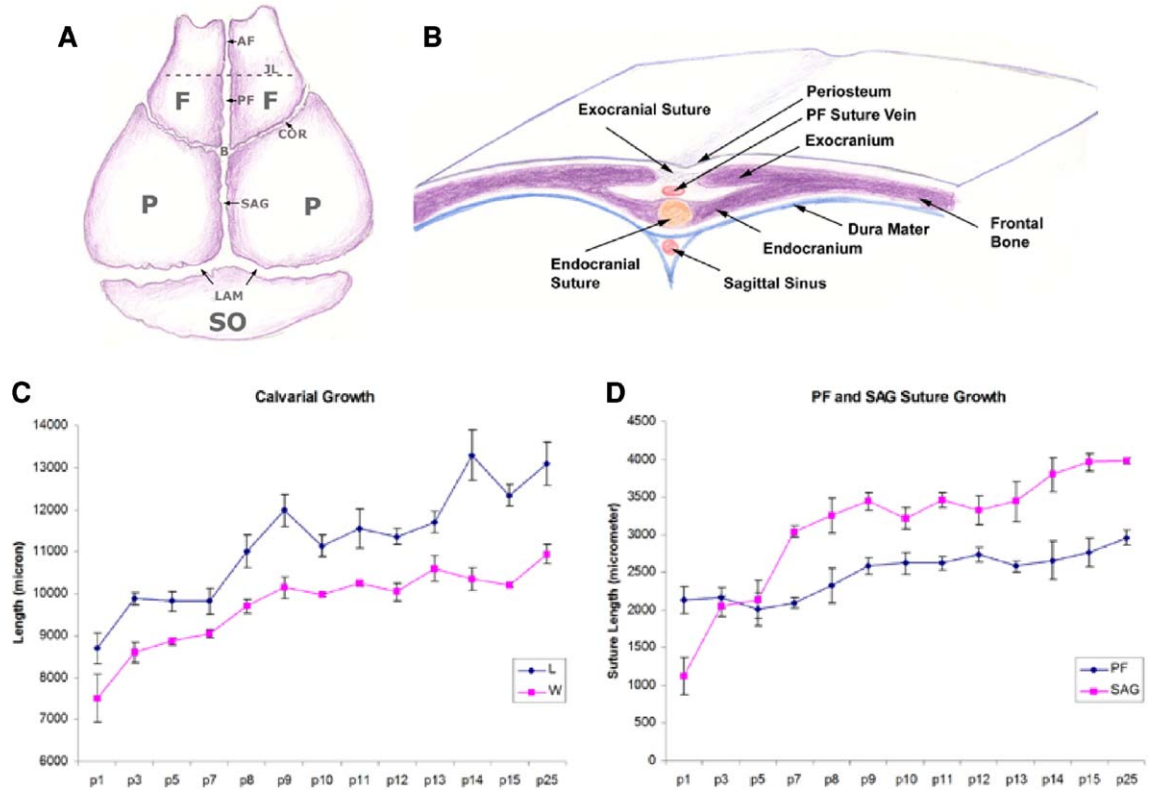

Fig. 1. Calvarial and suture development during the first month of life. A, drawing of skull vault anatomy, top view. This illustration depicts the components of skull vault. (F, frontal bone; P, parietal bone; SO, supraoccipital bone) The posterior frontal (PF) suture is situated between the frontal bones, posteriorly to the anterior frontal suture (AF), and anteriorly to the sagittal suture (SAG). Jugum limitans (JL) and bregma (B) are anatomical landmarks of PF suture. B, schematic representation of a skull vault section and PF suture architecture. C, calvarial development during the first month of life. Calvarial length (L) and width (W) growth is greatest during the first 9 days of life. D, PF and SAG suture growth during the first month of life. PF suture growth is relatively steady throughout the first month of life (32 μm/day), while the SAG suture grows in two phases. During the first one and half week of life, the growth is rapid (245 μm/day), followed by a moderate rate of growth (35 μm/day) similar to that of PF suture.

encompassing the sutures. The anterior landmark for the PF suture is the jugum limitans. The posterior landmark for the PF suture, as well as the anterior landmark for the SAG suture is the bregma, where COR suture transects between the PF and SAG sutures. The posterior landmark for the SAG suture is the lambdoidal suture (see Fig. 1A).

As it turns out, the PF suture growth is relatively steady during the growth of calvaria throughout the first month of life. However, the SAG suture grows rapidly before closure of the PF suture, then it slows down to a rate similar to the PF suture after closure is initiated. There is a temporal relationship between PF closure and growth rate of the SAG suture (pre and post closure rate). The PF suture is longer (24% of calvarial length at p1) than the SAG suture (13% of calvarial length at p1) during the first 5 days of life; however, this relationship changes quickly after the first 5 days of life due to rapid growth of the SAG suture during this period. The PF suture length contributes significantly to the length of the calvaria during the first 5 days of life. After the first 5 days of life, the SAG suture contributes more as its growth exceeds that of the PF suture (Fig. 1D).

The PF suture length postnatally ranges from 2 mm on p1 to 3 mm on p25, while the SAG suture ranges from 1.2 mm to approximately 4 mm during the same period. Moreover, during the first 2 weeks of life, the intrinsic growth of PF suture increases approximately by 25%, while the intrinsic growth of SAG suture increases approximately by 340% (data not shown).

Since the PF suture is the only calvarial suture in mice that closes during the first month of life, we next investigated the precise window of time when closure takes place, in order to analyze the expression profile and potential functional role of select neural crest determinant genes. Because histology is a successful technique for assessing cranial suture morphology and fate, serial coronal sections of PF sutures were obtained during the first month of life for detailed examination of this suture. As seen in Fig. 2A, evidence of PF suture changes preceding closure was seen as early as p7 in the form of cellular condensation in suture mesenchyme. However, an overt ossified bony bridge was not seen until p9–p10. This process started anteriorly in the PF endocranial layer and proceeded posteriorly. PF suture closure was largely completed by p15. Importantly, the ectocranial layer of PF suture remained patent out to the end of our study, time point (p25), and beyond (p240) (data not shown).

The timing of the mice PF closure presented here is earlier than what was previously reported (Bradley et al., 1996). A likely explanation for this discrepancy in timing lies in the nature of PF suture: intermittent points of closure alternate with patency areas, resulting in regions where the PF suture has closed and regions where it remains open (Fig. 4B).

PF suture development is unique

The difference between the PF suture and other cranial sutures goes beyond embryonic tissue origin. Although previous studies have treated the PF suture as either closing or non-closing (Bradley et al., 1996; Moss, 1958; Opperman, 2000), detailed studies of this suture revealed a more sophisticated architecture. The PF suture is comprised of a double layer interface stacked on top of each other: the ectocranial and endocranial layers (Fig. 2B). Our observation is in agreement with a study performed by Moss on rat PF sutures. Moss in his early histological study on PF sutural closure, described the following: "Ect- and endocranial plates of bone were clearly discernible. The sutural edges of the thin lamellar ectocranial plates of the frontal never fused" (Moss, 1958). All other cranial sutures, including SAG and COR sutures, form a single sutural interface between approaching calvarial plates (Fig. 2B). The ectocranial layer, overlying the endocranial layer, consists of a fibrous suture mesenchyme, the osteogenic fronts and the overlying periosteum. This layer, which can be seen from top view of skull (Fig. 1B), is contiguous with the SAG suture posteriorly at the bregma and the AF suture anteriorly at the landmark line, jugum limitans. Similar to SAG and COR sutures, the PF ectocranial layer remains patent throughout life. What makes the PF suture unique is the endocranial layer (Fig. 2B). Importantly, as shown in Fig. 2B, the closing endocranial PF layer is not present in both SAG or in COR sutures, which are known to be patent throughout life. Another difference between the PF, SAG and COR sutures is the presence of suture vein between the ectocranial and endocranial layers (Fig. 1B).

Histochemistry analysis of PF suture performed on embryos revealed at E14 only the presence of the sagittal sinus, while both the ectocranial and endocranial layers were not yet formed at this stage (Fig. 2C). At E18, the ectocranial layer was visible (Fig. 2D). In contrast, the endocranial layer and PF vein were not yet present at these stages (Fig. 2D). At p1, both ectocranial and endocranial layers of the PF suture were well defined, and the sagittal sinus was present, while the PF vein was still not visible (Fig. 2E). The PF vein was clearly detected between the approaching endocranial osteogenic fronts at p7 (Fig. 2F).

Neural crest markers Sox9 and Slug are upregulated during PF suture closure

The unique PF suture development described above was likely a result of differential gene expression at the suture complex level. Given the distinct neural crest origin of the PF suture complex, we asked what was the expression profile of NCC genes such *Sox9* and *Slug* during closure of the PF suture. After determining the precise timing of PF suture closure, we analyzed the expression profile of *Sox9* in the NCC-derived PF suture. We performed quantitative real-time PCR on the PF suture complex during the first month of life (Fig. 3A). Expression of *Sox9* was noted to increase by p7 and peak on p9/p10, before returning to baseline on p13. Next, to define the precise spatial localization of Sox9 protein during this time period, we performed immunohistochemistry using a Sox9-specific antibody on serially timed PF suture sections. As shown in Fig. 3B, nuclear localization of Sox9 protein was detected in the PF suture as early as p7. Maximal levels of Sox9 protein was observed on p9. Interestingly, Sox9 protein immunostaining was detected only on alternate sets of histological sections derived from the entire PF suture, and corresponding to regions undergoing closure.

To examine expression of *Slug* during PF suture closure, we performed quantitative real-time PCR followed by immunohistochemistry on PF suture during the time of closure using a Slug specific antibody. Our results indicated a maximal expression of *Slug* on p9 at both mRNA and protein levels (Figs. 3C and D).

Interestingly, no up-regulation of *Sox9* expression was noted at anytime during the first month of life in the SAG suture (Figs. 3E and G) as well as in the AF suture (data not shown). These results indicated that expression of *Sox9* tightly correlated with areas of suture closure, indeed suggesting a potential role of *Sox9* in PF suture closure. Unlike *Sox9*, however, up-regulation of *Slug* gene expression was observed in SAG suture at the time when PF suture closure occurs (Fig. 3F).

Fig. 2. Analysis of PF suture closing time and morphogenesis. A, H&E histochemistry analysis of PF suture from p1, p5, p9, p11, p13, p15, p17, p25 reveals bony closure during the second week of life. The PF suture mesenchyme (arrow, p1) in mice undergoes initial closure between p9 and p11 and completes this process by p15–17. Note, only the endocranial layer of PF suture is closed by p25 (arrow), while the ectocranial layer (arrowhead) is still open. This layer remains patent throughout life-time (data not shown). B, comparative structural analysis of PF, SAG and COR suture at p9. The PF suture complex is comprised of two (endocranial and ectocranial) layers separated by a vein and connective tissues, while both SAG and COR suture form a single layer between the approaching cranial plates. C, H&E histochemistry analysis of PF suture from E14 reveals only the presence of the sagittal sinus. D, at E18, the ectocranial layer of PF suture is detected (right columns represent higher magnification of the suture sections). E, at p1, both ectocranial and endocranial layers of the PF suture are well defined, while the PF vein is not yet detected. F, at p7, the PF vein is clearly visible between the approaching endocranial osteogenic fronts. Abbreviations used: (F, frontal bone; OFs, osteogenic fronts; PFect, PF ectocranial layer; PFend, PF endocranial layer; P, parietal; M, mesenchyme; PO, periosteum; DM, dura-mater; SS, sagittal sinus; PSV, PF suture vein) (magnification at 63×).

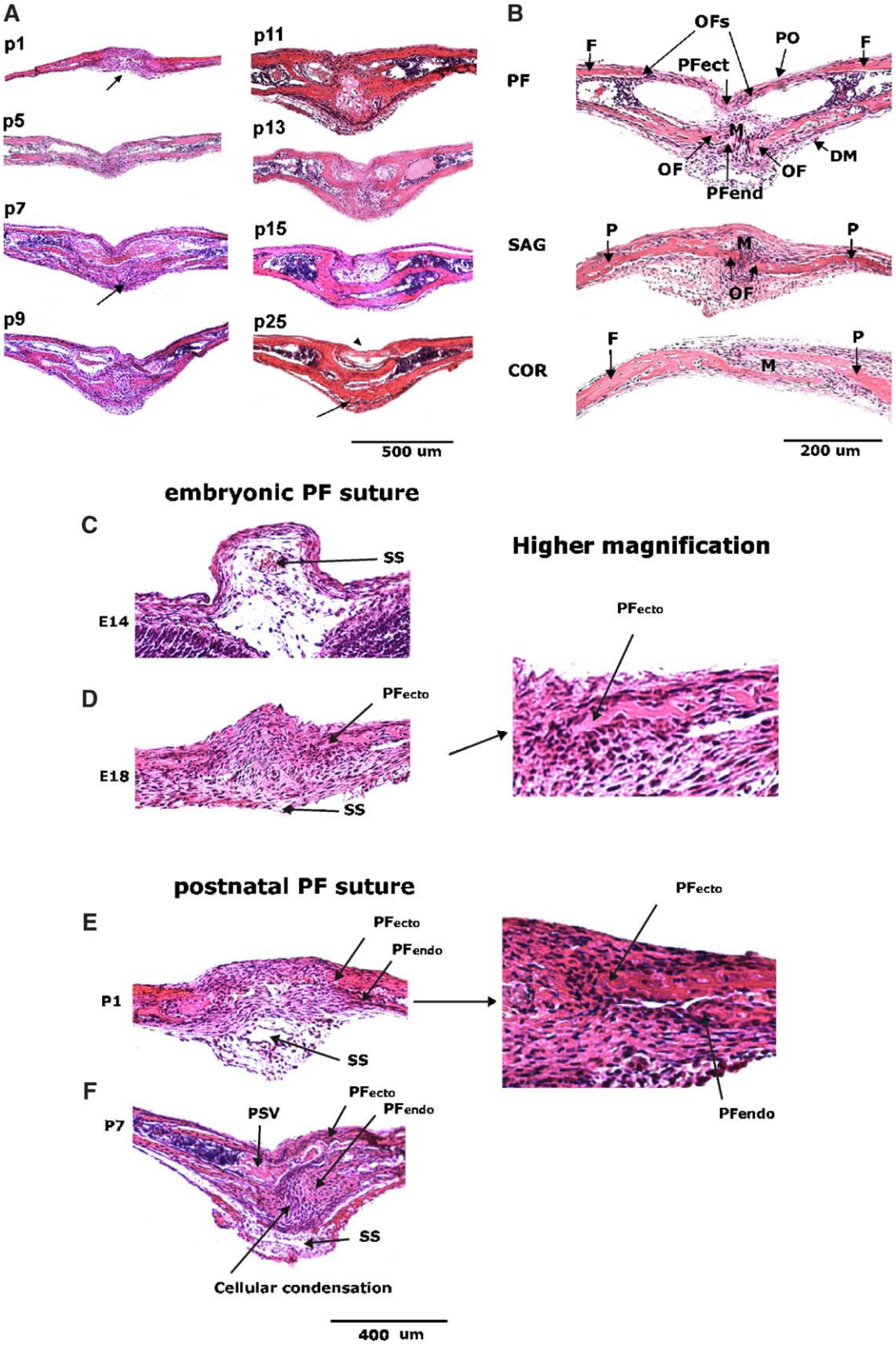
A
p1
p5
p7
p9
p11
p13
p15
p25
500 um
B
PF
SAG
COR
OFs
PO
F
PFect
M
OF
DM
PFend
P
200 um
embryonic PF suture
C
SS
E14
Higher magnification
PFecto
D
E18
postnatal PF suture
E
P1
PFendo
F
P7
PSV
Cellular condensation
400 um

Sox9 gene expression domains control chondrogenesis in PF suture

In addition to its neural crest determining role, *Sox9* is also a master regulator of chondrogenesis (Akiyama et al., 2002; Bi et al., 2001; de Crombrugghe et al., 2000; Mori-Akiyama et al., 2003; Wright et al., 1995). The presence of *Sox9* expression in the PF suture during closure suggested chondrogenesis might be taking place. To verify this possibility, we analyzed serial sections of PF suture using Safranin-O staining which detects negatively charged glycosaminoglycan (GAG) production (Fig. 4A). Cell condensation, a process preceding chondrogenesis (Haas and Tuan, 1999), was noted within the mesenchyme of the endocranial layer of the PF suture as early as p7, while overt maximal chondrogenesis and Safranin-O-positive staining was observed between p8 and p9, followed by hypertrophy of chondrocytes at p10 (Fig. 4A). Minimal, if any, cartilaginous tissue was noted by p13. No cartilage formation was noted in the ectocranial layer of PF suture during this time. Immunohistochemistry using Sox9 antibody detected, as expected, co-localization of Sox9 protein in the areas of chondrogenesis. Intriguingly, chondrogenesis, as well as Sox9 protein immunostaining was detected only on alternate sets of histological sections derived from the entire PF suture. This observation suggested that chondrogenesis might not be occurring through the entire region of the PF suture.

To verify this possibility, Alcian blue staining of whole-mount calvaria was performed to analyze chondrogenesis in the calvaria skull vault (Fig. 4B). Initial chondrogenesis domains were observed anteriorly in the PF suture at points of contact (joints) between the approaching frontal bones as early as p8. By p9, multiple centers of chondrogenesis were seen anteriorly followed by closure of the suture and loss of cartilage by p11–p12. Thus, chondrogenesis was not present throughout the entire PF suture, rather it was noted in intermittent areas alternated with areas of patency (gaps) which were negative for Alcian blue staining. To examine also the expression of *Sox9* and its target gene *Col II* in these patent areas (gaps) of PF sutures, we performed immunohistochemistry on sections derived from these areas using a Sox9 specific antibody (Fig. 4C). No Sox9 or Type II Collagen protein was detected in these areas, thus confirming the presence of *Sox9* and chondrogenesis associated with area of PF suture closure and not areas of suture patency.

Sox9 regulates the expression of cartilage specific extracellular matrix molecules, Type II Collagen (Col II) (Bell et al., 1997; Lefebvre et al., 1997) and Type X Collagen (Col X) (Zehentner et al., 1999). To confirm this relationship in the closing PF suture complex, quantitative real-time PCR was performed for both of these extracellular matrix molecule genes. *Col II* and *Col X* expression was maximal on p9 and p10, respectively (Figs. 5A and C). While *Col II* returned to baseline by p11, *Col X* remained high on this time point and returned to baseline by p13. This temporal *Col X* expression pattern is consistent with its known pattern of expression in hypertrophic cartilage. To analyze Col II and Col X protein levels in closing PF sutures, we performed immunohistochemistry on PF sutures at serial time points using Col II- and Col X-specific antibodies. Col II and Col X proteins (Figs. 5B and D) were localized to the endocranial layer of PF sutures on p9 and p10, corresponding to their transcriptional expression time points. Taken together, these data indicated chondrogenesis in the endocranial layer of PF sutures prior to closure.

PF suture closes through endochondral ossification

To assess the fate of cartilage present in the PF suture and verify possible endochondral ossification occurring during PF suture closure, we analyzed the expression of bone markers *Type I Collagen* (*Col I*) and *Osteocalcin* in the PF suture complex. During the first week of life where rapid growth of skull was observed, *Col I* was up-regulated (Fig. 6A). Upon onset of closure of PF suture and chondrogenesis, *Col I* was sharply down-regulated, but was up-regulated again during ossification of the PF suture with peak expression on p13, returning to baseline by p17. *Osteocalcin*, a marker of terminally differentiated osteoblasts, was maximally expressed during the late period of PF suture closure (Fig. 6B). An increase in *Osteocalcin* expression was noted on p13 with maximum expression on p15, returning to baseline by p17. We performed immunohistochemistry using Osteocalcin specific antibody to detect the corresponding level of Osteocalcin protein product. In the PF suture up to p9, a low amount of Osteocalcin staining was seen between the osteogenic fronts (Fig. 6C). Starting with p11, this area revealed increased Osteocalcin protein staining. By p13 the intensity of Osteocalcin immunostaining in the PF suture was equivalent to the surrounding bony structures signifying a complete bony bridge between the osteogenic fronts. Thus, the expression of both *Col I* and *Osteocalcin* in the same area of PF suture where we previously showed cartilage formation, strongly suggested the occurrence of endochondral ossification of this suture.

Expression of Fgf-2 and Fgf-18 during suture closure

The observation of unique *Sox9* expression as well as chondrogenesis during initiation of PF suture fusion prompted us to investigate the expression of potential regulators of *Sox9* gene during the period of suture closure. Murakami et al. (2000) demonstrated a MAP kinase mediated *Sox9* up-regulation by FGF-2 in chondrocytes and undifferentiated mesenchymal cultured cells. Moreover, in vitro studies showed chondrogenic differentiation of premigratory NCC with exogenous FGF-2 stimulation (Sarkar et al., 2001). On the contrary, FGF-18, a regulator of cell proliferation and differentiation, negatively affects chondrogenesis while positively affecting osteogenesis (Ohbayashi et al., 2004). Since the NCC-derived PF suture complex undergoes transient chondrogenesis followed by osteogenesis, we

investigated whether *Fgf-2* gene expression would temporally coincide with the chondrogenesis phase, while *Fgf-18* gene expression would coincide with the osteogenesis phase of PF suture closure. To address this question, we analyzed the expression of *Fgf-2* and *Fgf-18* in the PF suture complex during the first month of life using quantitative real-time PCR. Interestingly, we observed that *Fgf-2* and *Sox9* genes were temporally co-expressed in the PF suture complex. Maximum expression of *Fgf-2* was observed on p9, a time when expression of *Sox9* and chondrogenesis occurred (Fig. 7A). Only baseline expression of *Fgf-2* was noted in SAG suture during the same period (Fig. 7C). These results demonstrated temporal co-expression of *Fgf-2*, a potential regulator of *Sox9* and chondrogenesis in the PF suture. In contrast, an increased level of *Fgf-18* expression was observed on p11–p13, the most active period of suture

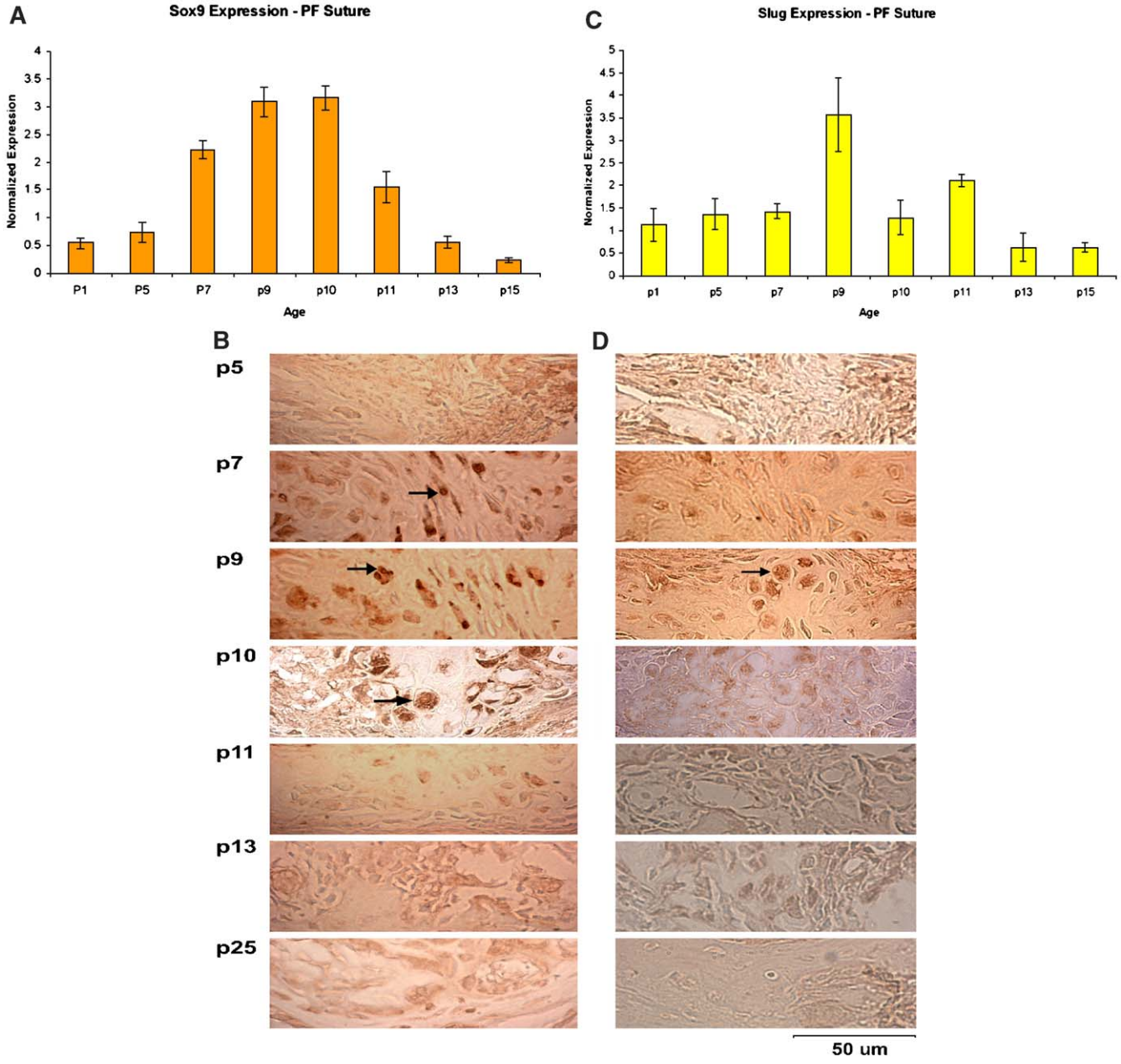

Fig. 3. Neural crest cell determinant *Sox9* and *Slug* gene expression during PF suture closure. A, quantitative real-time PCR on PF suture complex performed at different time points shows an upregulation of *Sox9* as early as p7 with maximum expression on p9–p10 with return to baseline by p13. B, immunohistochemistry analysis performed using specific a Sox 9 antibody reveals localization of Sox 9 protein in the nucleus of the PF endocranial sutural cells on p7 and p9 (arrows). Only residual expression is noted on p11 and no expression by p13. C, quantitative real-time PCR for *Slug* on PF suture complex reveals upregulation of *Slug* expression maximal on p9. D, immunolocalization of *Slug* protein using a specific *Slug* antibody reveals *Slug* protein in the PF endocranial suture mesenchymal cells on p9, with minimal expression on p7 and p10. E–G, *Sox9* and *Slug* expression in SAG suture. E, quantitative real-time PCR and G, immunohistochemistry shows only baseline expression of *Sox9* in the SAG suture during the first month of life. F, quantitative real-time PCR shows upregulation of *Slug* expression on p9 (magnification at 63×).

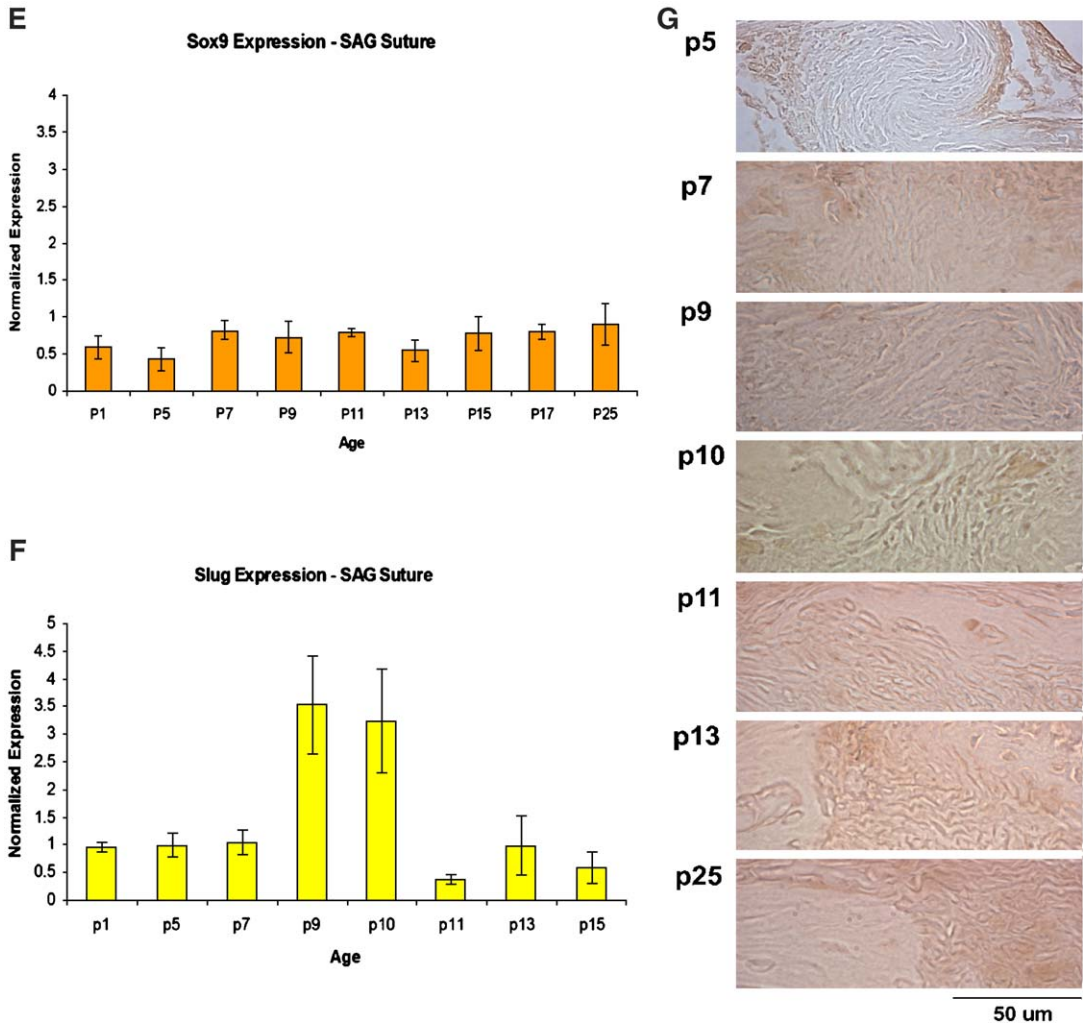

Fig. 3 (*continued*).

closure and osteogenesis (Fig. 7B). *Fgf-18* expression was decreased by p15, when closure was mostly completed. These results demonstrated that members of the FGF family which are known as positive regulators of both chondrogenesis and osteogenesis are expressed in a temporo-spatial pattern consistent with the PF suture closure. Therefore, we speculate that FGF-2 may control the expression of *Sox9* and chondrogenesis during PF suture closure, whereas FGF-18 may control osteogenesis.

The diagram in Fig. 7D summarizes the temporal gene expression profiles and differentiation events occurring during the closure of PF suture.

Analysis of PF suture phenotype in Sox9 conditional knock-out mice

Because of the unique and controlled expression pattern of *Sox9* gene at both message and protein levels during PF suture closure we sought to determine whether *Sox9* could play a role in PF suture closure. Indeed, we investigated whether a depletion of cartilage formation would affect the fate of PF suture closure. To answer our question we analyzed the PF suture phenotype in *Sox9*-deficient mice in vivo. This analysis would give us insight into the functional importance of *Sox9* during PF suture closure. Homozygous or heterozygous loss of function mutations in *Sox9* gene are not compatible with life (Bi et al., 2001). Therefore, we used the *Cre recombinase/loxP* (*Cre/loxP*) system (Gu et al., 1994) to develop a *Sox9*-insufficient state selectively in NCC derived tissues using mice harboring *Wnt1-Cre* transgene and a floxed *Sox9* allele (Akiyama et al., 2002). Since complete loss of *Sox9* in NCC-derived tissue is lethal perinatally (Mori-Akiyama et al., 2003), this mutant would preclude our study which requires survival during the first 2 weeks of life. However, haploinsufficiency of *Sox9* in NCC derived tissue is viable (Mori-Akiyama et al., 2003). We obtained haploinsufficient $Sox9^{flox/WT;Wnt1\text{-}Cre}$ mice by crossing $Sox9^{flox/WT}$ female mice with *Wnt1-Cre* male mice (Fig. 8A). Heterozygotic mice harboring $Sox9^{flox/WT;Wnt1\text{-}Cre}$ were viable and fertile, although with significant perinatal mortality compared to controls. $Sox9^{flox/WT;Wnt1\text{-}Cre}$ and control littermates were sacrificed on p10, the onset of PF

suture closure. Whole fresh calvariae of mutant mice examined under *a* stereo-microscope revealed hypoplastic craniofacial skeleton and a smaller domed shape skull (Fig. 8A). The PF cranial sutures in mutants were grossly patent, as seen under low power field in Fig. 8A, while control groups had already began the process of closure by forming points of contact anteriorly. We then analyzed the p10 PF suture complex sections using H&E and Safranin-O staining. In mutant mice (n = 12), the endocranial layer of PF suture was widely patent on p10, while the WT group (n =

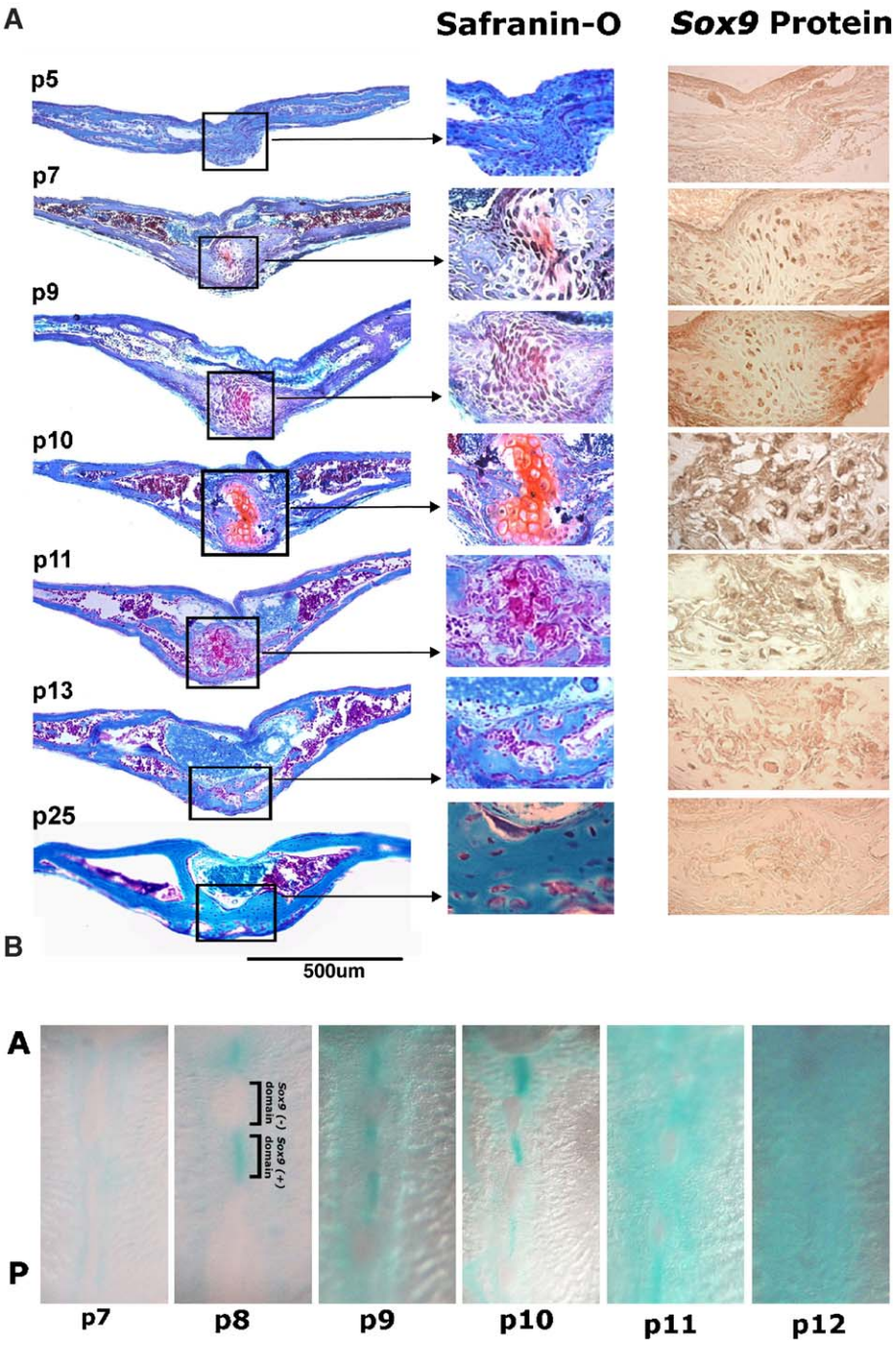

Fig. 4. Chondrogenesis precedes PF suture closure. A, histological analysis of the PF suture obtained from specific areas (joint repeats) of PF suture using Safranin-O staining revealed proteoglycan staining of the PF suture evident as early as p7–p8 and peak on p10. No staining is detected by p13. (Middle column represents higher magnification of the boxed areas). Note, co-localization of proteoglycan staining with Sox 9 protein in the area of condensing endocranial mesenchymal cells in the PF suture between osteogenic fronts. B, Alcian blue staining of whole-mount calvariae reveals initial points of chondrogenesis visible as early as p8 on the anterior part (A) of the PF suture. More areas of chondrogenesis are noted on subsequent days with peak between p9 and p10 in the posterior part (*P*) of the PF suture. C, immunohistochemistry analysis of tissue sections derived from the patent areas (gap repeats) of PF suture on p7 and p9 does not reveal any *Sox 9* protein as well product of its target gene *Col II*.

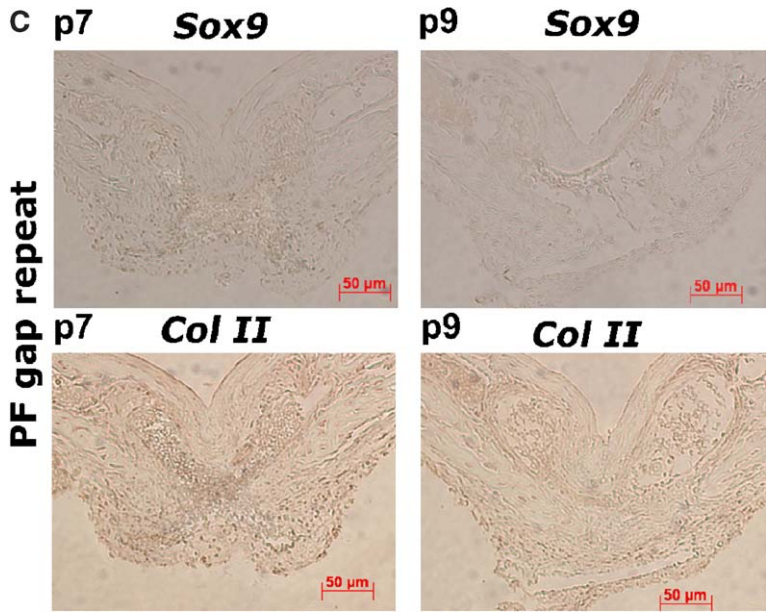

Fig. 4 (*continued*).

12) exhibited initiation of closure through thickening and chondrogenesis (Fig. 8B). There was also a decrease in calvarial bone thickness, especially in the PF suture area, compared to the WT mice. By p15 complete closure of PF suture was observed in WT mice (n = 6). In contrast, $Sox9^{flox/WT;Wnt1\text{-}Cre}$ mice (n = 7) still showed lack of PF suture closure. These results were seen in over 90% of $Sox9^{flox/WT;Wnt1\text{-}Cre}$ mutants indicating a high penetrance of this phenotype. However, histological analysis of PF suture in older animals (p35) showed only an impaired closure of PF suture for $Sox9^{flox/WT;Wnt1\text{-}Cre}$ mutant mice (data not shown). In addition, we performed Alcian blue staining of whole-mount calvariae on $Sox9^{flox/WT;Wnt1\text{-}Cre}$ to analyze the patterning of chondrogenic domains within the PF suture previously observed in WT mice (Fig. 4B). As shown in Fig. 8C at p9, the timing when multiple chondrogenic domains are present in WT mice, none of these domains where detected in $Sox9^{flox/WT;Wnt1\text{-}Cre}$ mice during the same time points. Thus, in $Sox9^{flox/WT;Wnt1\text{-}Cre}$ mutant mice, the distinct patterning of PF suture preceding its closure was lost. Taken together, the above results suggest an important role for *Sox9* in PF suture patterning and timing of closure.

Discussion

Calvaria origin can be traced back to neural crest and paraxial mesoderm. The frontal bone plates and the PF suture (analogous to metopic suture in human) originate from NCC in vertebrates (Couly et al., 1993; Jiang et al., 2002; Le Lievre, 1978; Morriss-Kay, 2001; Noden, 1975). Thus, the PF suture is the only suture derived solely from the NCC and flanked by calvarial plates on both sides derived from NCC. Since this is the only cranial suture that closes during the lifetime of mice, it warrants the question of whether the unique origin of this suture complex is responsible for its unique fate. To date, no analytical study of PF suture development in mice has been reported. In this study, we have analyzed the morphogenesis and events related to the closure of posterior frontal (PF) suture in mice. Using the PF sutural complex as a model system, we investigated the timing and morphological changes leading to suture closure as well the expression and functional role of the neural crest determinant gene *Sox9* during suture closure.

Biological significance of neural crest determinant genes Slug and Sox9 expression in the PF suture

Much attention has been given to the expression of several genes in coronal and sagittal sutures, including FGF receptors and ligands, BMP ligands, transcription factors *Msx* and *Twist* (Kim et al., 1998; Liu et al., 1999; Rice et al., 2000). Because of its entirely neural crest origin, we analyzed the expression of NCC determinant genes *Slug* and *Sox9* in the PF cranial suture during the time when the suture closure occurs. The expression analysis demonstrated that there was a unique expression profile for *Sox9* gene in the PF suture during the time of closure.

This observation is particularly interesting and would suggest that *Sox9* plays a unique and perhaps essential role in the development and fate of the PF suture. Furthermore, the differential expression of *Sox9* in the PF cranial suture indicates execution of a distinct morphogenetic program for this suture. Analysis of whole-mount skulls stained with Alcian blue revealed that the pattern of closure of the PF suture is characterized by the presence of areas of closure alternated with areas of patency ("joint-gap" repeats), where closure areas are marked by *Sox9* gene expression as well as

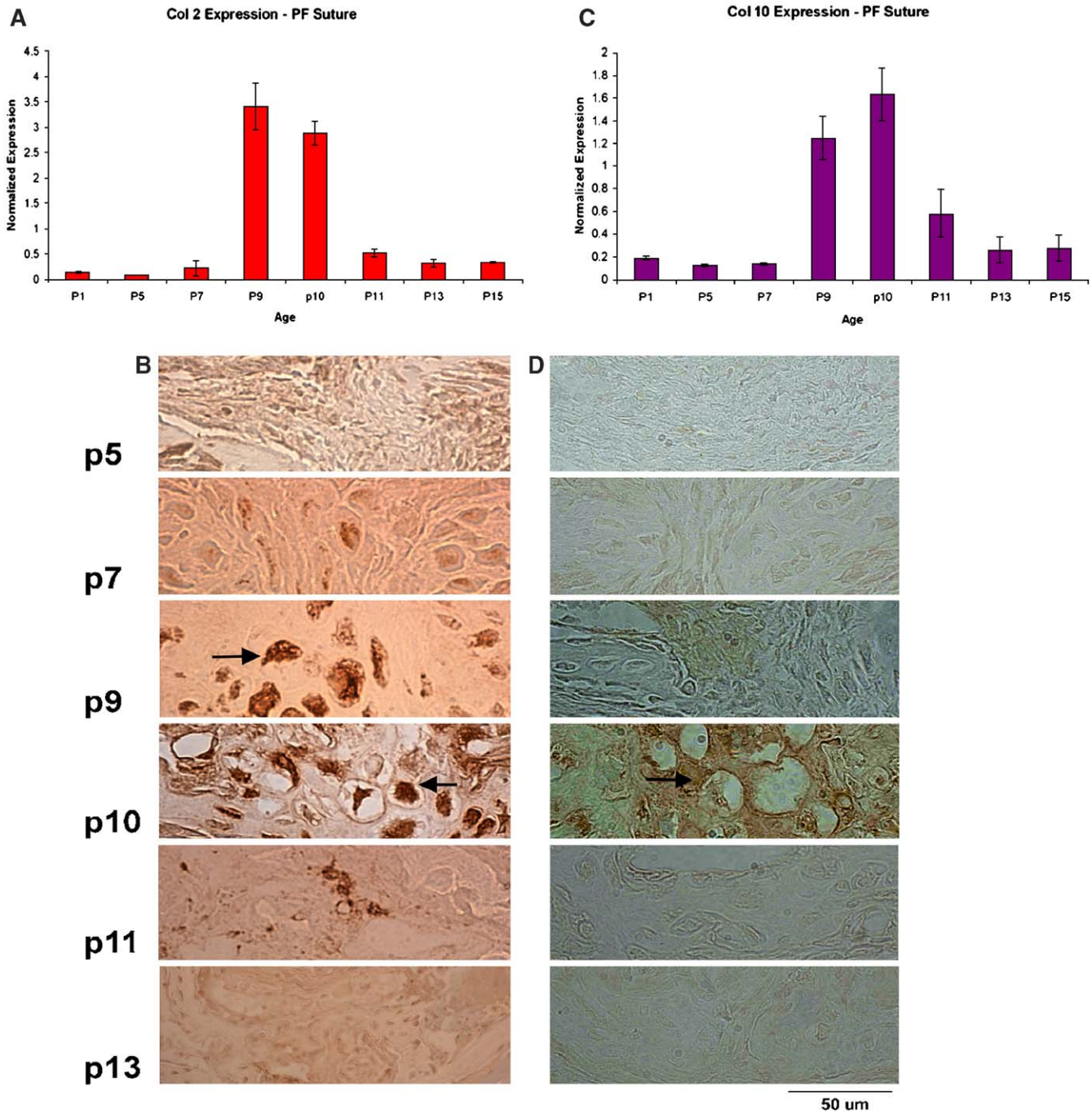

Fig. 5. Expression of cartilage markers *Col II* and *Col X* in the PF suture complex. A, quantitative real-time PCR shows that *Col II* expression was maximal on p9 with return to baseline by p11. B, immunohistochemistry shows maximum type II collagen protein on p10. Starting from p11 type II collagen immunostaining decreased. No protein was detected by p13. C, quantitative real-time PCR showed *Col X* expression was maximal on p10 with return to baseline by p13. D, immunohistochemistry showed maximum type X collagen protein antigen by p10 in the endocranial mesenchyme of PF suture with residual amount on p13 (magnification at 63×).

cartilage positive domains. We believe that the "unique" recapitulation of *Sox9* during the time of PF suture is of biological importance and sets up the conditions for endochondral ossification leading to PF suture closure, as haploinsufficiency of *Sox9* gene caused a delay in suture closure due to impaired cartilage formation. We hypothesize that the upregulated expression of *Sox9* within the suture mesenchyme prior to PF suture closure directs a differentiation decision, biasing neural crest cells toward chondrocytes. In support of this hypothesis is the recent work by Cheung and Briscoe (2003) which demonstrated that neural crest development is regulated by *Sox9* and that *Sox9* acts at two stages of neural crest differentiation: first as an intrinsic determinant of neural crest, initiating neural crest develop-

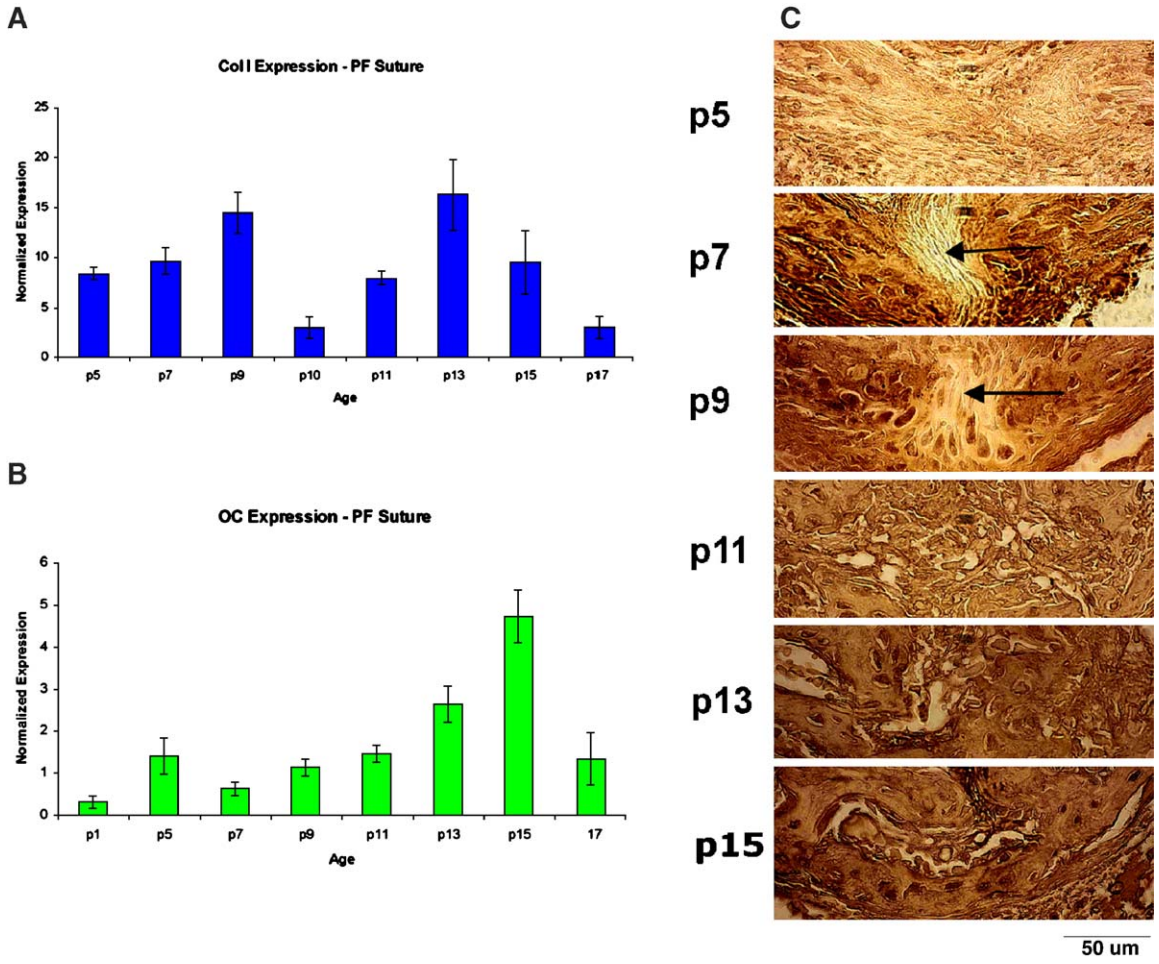

Fig. 6. Expression of bone markers in PF suture. A, quantitative real-time PCR shows expression of *Col I* to be elevated during the first 9 days of life. *Col I* is downregulated sharply on p10, then upregulated with maximal expression by p13 with return to baseline by p17. B, quantitative real-time PCR shows that *Osteocalcin* expression is upregulated during closure of PF suture. It is first seen upregulated by p13 with maximal expression by p15 and return to baseline by p17. C, immunohistochemistry analysis of Osteocalcin protein on the endocranial layer of the PF suture shows presence of this protein as early as p11. Osteocalcin protein level increases by p13, a period of active bone deposition in the endocranial area of PF suture Note clear areas (arrow) between the osteogenic fronts (p7 and p9), where suture mesenchyme has not yet been ossified (magnification at 63×).

ment and segregating this lineage from neuroepithelium, and subsequently directing differentiation decisions in the periphery, biasing neural crest cells to glial cell and melanocyte lineages and away from neuronal fate. We believe that the expression of *Sox9* in the mesenchymal cells within the PF suture area leads to their differentiation into chondrocytes, and therefore, the PF suture closes eventually through an endochondral ossification process. Therefore, we propose that the PF suture closure may be controlled during postnatal calvarial development by the up-regulation of neural crest determinant gene *Sox9* which promotes cartilage formation as an intermediate step preceding calcification and bony bridge formation defining suture closure. It is likely that *Sox9* specifies the mesenchymal cells in the PF suture to became cartilage, but what are the factors responsible for the unique induction of *Sox9* expression in this region of calvarial suture? What is the signaling pathway triggering the up-regulation of *Sox9*? Is there positional information that instructs neural crest-derived cells present in the PF suture to up-regulate *Sox9* gene expression, or is there an intrinsic capacity of these specific neural crest-derived cells to recapitulate the expression of *Sox9*? Why do mesenchymal neural crest-derived cells present within the SAG suture, which remains patent throughout life, not express *Sox9* gene although they express other neural crest determinant genes such as *Slug*? These are all challenging, as well as fascinating questions that deserve answers. The fact that only the neural crest-derived cells within the PF suture are able to recapitulate the expression of *Sox9* gene would suggest that positional inductive signal(s) rather than a cell-autonomous event is responsible for the unique expression of *Sox9* in the PF suture. It is known that various members of the FGF superfamily, in particular FGF-2 up-regulates the expression of *Sox9* in chondrocytes (Murakami et al., 2000). Our data demonstrate a co-expression of *Fgf-2* and *Sox9* within the PF suture. In contrast, *Fgf-2* is not expressed at the same time points in the SAG suture. In light of these results, it is

tempting to speculate that FGF-2 may be one of candidate molecules controlling the expression of *Sox9* gene during PF suture closure.

Posterior frontal suture closure occurs through endochondral ossification

Bone development occurs by intramembranous or endochondral ossification. Intramembranous ossification involves direct osteogenesis from mesenchymal cells without the intermediate participation of cartilage. In contrast, endochondral ossification occurs within a cartilage model in which chondrocytes undergo hypertrophy and apoptosis and are replaced by invading osteogenic cells. The PF suture is formed between intramembranous NCC-derived frontal bones. Our study demonstrated that the PF suture undergoes fusion through a process of endochondral ossification as demonstrated by the expression profile of several genes. It is well established that in vivo, the chondrogenic lineage is specified by the transcription factor *Sox9*, the expression of which is necessarily required for cartilage formation (Akiyama et al., 2002; Bi et al., 2001; Mori-Akiyama et al., 2003). By binding to specific target enhancers on cartilage markers (Type II, IX, and X), CD-RAP and aggrecan, Sox 9 protein induces the expression of a chondrocyte phenotype at the early stage of condensation of mesenchymal precursors, which is fundamental to the onset of chondrogenesis (de Crombrugghe et al., 2000). As a first index of chondrogenicity, we have shown expression of *Sox9*, a marker of precartilage condensation (Ng et al., 1997; Zhao et al., 1997) as well as *type I collagen*, a molecular marker of undifferentiated chondroprogenitors (Kosher et al., 1986; von der Mark, 1980). Subsequently, the complete absence of *type I collagen*, together with high level of *type II collagen*, indicated that the chondrocytes were differentiating in the PF suture prior to closure. Moreover, these differentiated chondrocytes then sustained a series of sequential changes that included conversion to hypertrophic chondrocytes expressing high levels of *type X collagen*. Furthermore, osteogenesis, as shown by the expression of both *type I collagen* and *Osteocalcin*, markers of bone formation, further supported an endochondral ossification within the PF suture. Therefore, we conclude that the cartilage detected within the PF suture is subsequently replaced by bony tissue. However, whether the entire cell population or a small subset of neural crest-derived cells adopt the chondrogenic fate is unknown.

Several questions can be raised from our current work. First, does the endochondral ossification control the entire process of PF suture closure? Second, is the endochondral ossification an evolutionarily conserved pattern of PF suture closure? In rats as well as humans, presence of cartilage tissue in the PF suture before the time of closure has been reported (Manzanares et al., 1988; Moss, 1958). Interestingly, in zebrafish where the PF suture stays patent throughout lifetime, there is no evidence of cartilage formation within the PF suture (Quarto, N., unpublished results). These findings suggest that endochondral ossification during PF suture closure may be a unique feature of mammalian organisms,

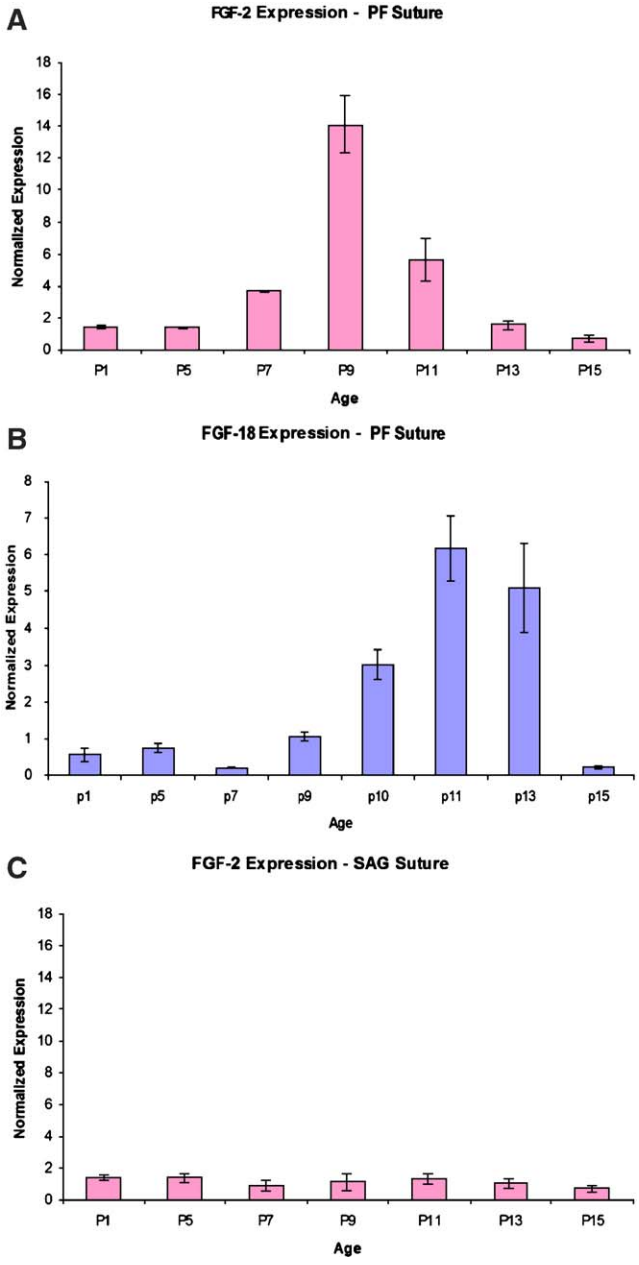

Fig. 7. *Fgf-2* and *Fgf-18* expression profile in PF suture complex. A, quantitative real-time PCR revealed a peak of *Fgf-2* expression on p9, coinciding with maximum *Sox9* peak expression. Expression returned to baseline by p13. B, quantitative real-time PCR reveals an up-regulation of *Fgf-18* gene expression starting on p10, the onset of sutural ossification. Maximum expression is seen on p11–13, a period coinciding with a period of maximal bone deposition for suture closure. Only background expression of *Fgf-18* was seen by p15, a period where suture closure was mostly completed. C, note, likely as described for *Sox9* gene expression in SAG suture (Fig. 3E), no upregulation of *Fgf-2* expression is detected in the SAG suture using quantitative real-time PCR. D, temporal expression of key genes involved in PF suture closure. The diagram summarizes the temporal gene expression profiles and differentiation events occurring during PF suture closure.

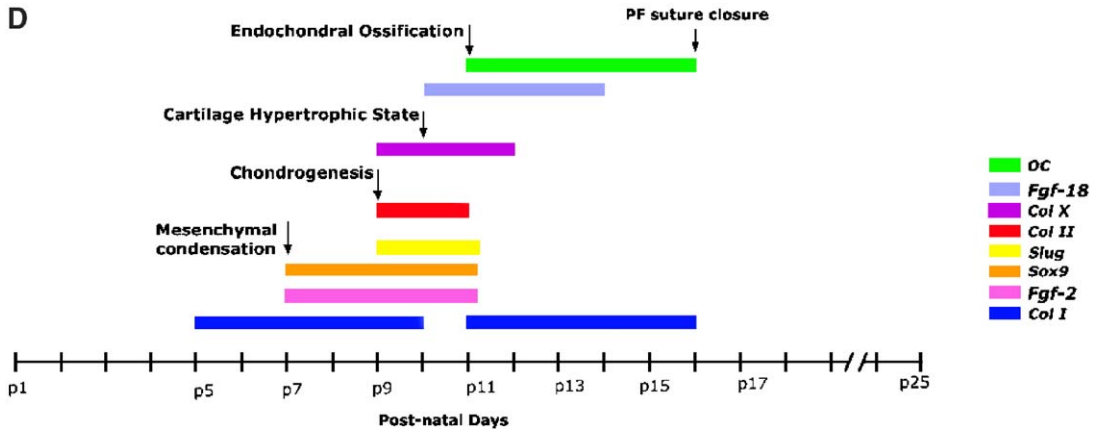

Fig. 7 (*continued*).

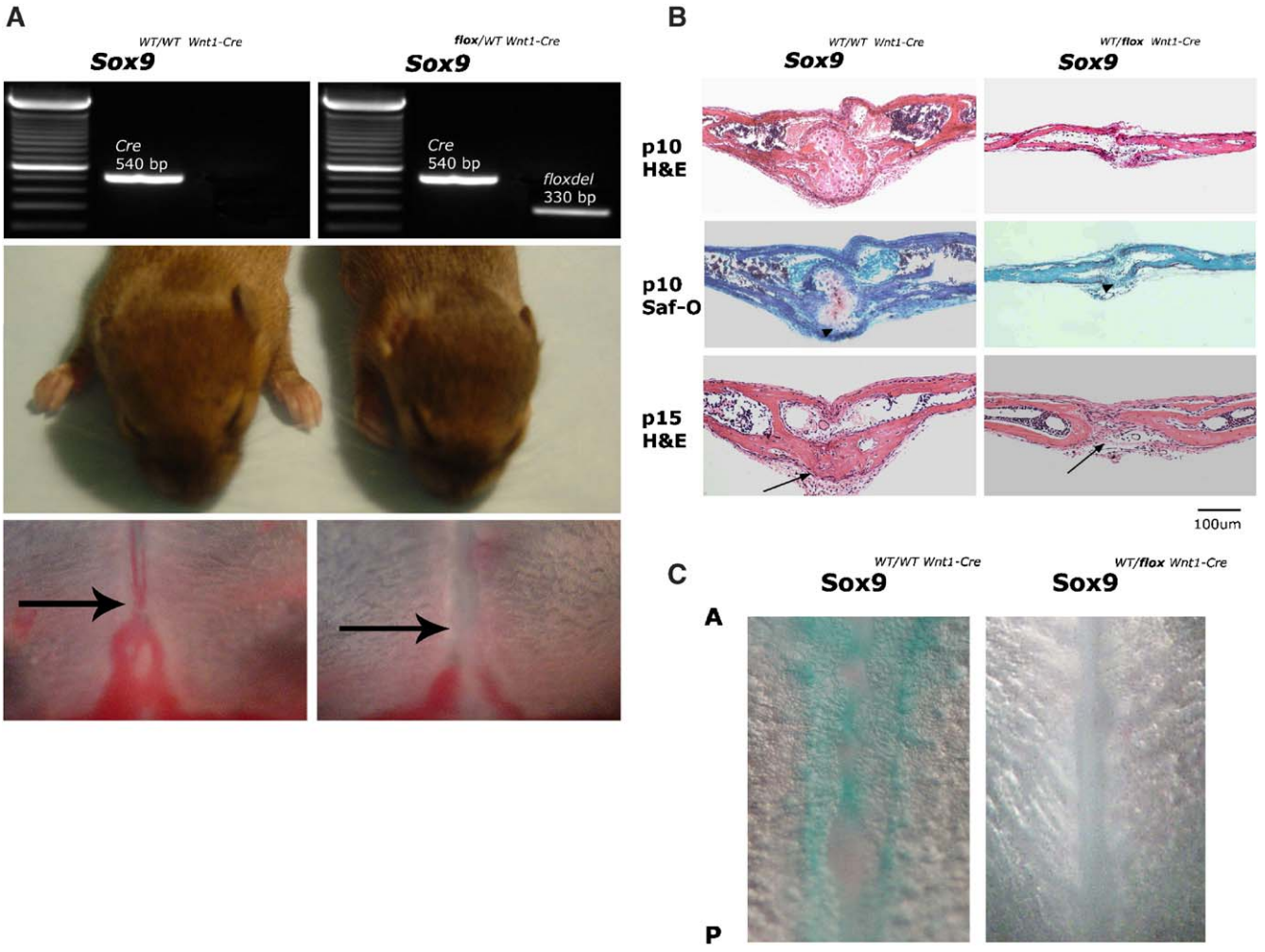

Fig. 8. Analysis of PF suture phenotype in *Sox9* conditional ko mice. A, $Sox9^{flox/WT;Wnt1\text{-}Cre}$ mice were generated by crossing $Sox9^{flox/WT}$ with *Wnt1-Cre* mice. Progeny were genotyped by PCR. Mice harboring $Sox9^{flox/WT;Wnt1\text{-}Cre}$ exhibited a hypoplastic craniofacial skeleton with smaller and domed shaped skulls. (Lower panel), fresh calvariae of p10 animals analyzed under stereo microscope (magnification 2.4×) reveals a patent PF suture in the mutant mice (arrow), while clearly showing areas of closure in the wild-type mice (arrow). B, H&E and Safranin-O staining of PF suture sections from p10 mice show an endochondral ossification in the wild-type, while in the mutant mice no area of chondrogenesis or osteogenesis is seen in the endocranial layer (arrowheads). By day p15, complete closure of PF suture is observed in wild type mice, whereas in $Sox9^{flox/WT;Wnt1\text{-}Cre}$ mutant mice PF suture is still open (arrows) (magnification at 63×). C, Alcian blue staining of whole-mount calvariae at p9 reveals chondrogenic domains in the PF suture of WT mice, while is noted absence of these domains in PF suture of $Sox9^{flox/WT;Wnt1\text{-}Cre}$ mice (A, anterior, P , posterior).

and that a chondrogenic event is a "prerequisite" for PF suture closure. In support of the latter hypothesis are our data showing the lack of chondrogenesis events in sagittal and coronal sutures that normally do not undergo closure.

Sox9 haploinsufficiency in cranial neural crest-derived cells impairs PF suture closure

Many craniofacial defects can be traced to abnormalities in neural crest biology. The neural crest is a transient migratory population of stem cells derived from the dorsal neural folds at the border between neural and non-neural ectoderm (Le Douarin and Kalcheim, 1999; Mayor et al., 1999). These unique cells are characterized by their extensive migration and ability to generate a large spectrum of cell types (Bronner-Fraser, 1994; LaBonne and Bronner-Fraser, 1999; Selleck et al., 1993).

The PF suture represents a mesenchymal structure of cranial neural crest (CNC) origin. Our initial data demonstrated a temporally-specific and unique up-regulation of *Sox9* in the PF suture mesenchyme during the time preceding suture closure. Moreover, the expression of *Sox9* was followed by cartilage formation and endochondral ossification. These observations prompted us to examine the potential role of this master regulator of chondrogenesis in the PF suture closure. We asked whether inactivation of *Sox9* could affect the proper timing and/or impair PF suture closure. For this purpose, we used *Wnt1-Cre Sox9^{flox}* conditional heterozygotic mice and analyzed the phenotype and the timing of PF suture closure. The *Wnt1-Cre Sox9* system has the advantage of distinguishing between neural crest-derived and mesodermal components of cranial skeletogenic mesenchyme and thus, to investigate the tissue origin of endochondral ossification.

In *Sox9* haploinsufficient mice, we observed a lack of suture closure when compared to the wild type mice. However, at later stages, an impaired PF suture closure was observed in *Sox9* haploinsufficient mice (data not shown), probably as result of a dosage-gene compensation. The observation that PF suture closure was impaired in the *Sox9* haploinsufficient mice, strongly indicated that *Sox9* is involved in suture closure, possibly by inducing cartilage formation that undergoes endochondral ossification, leading to suture closure. Based on these data, we speculate that a complete knock-out of *Sox9* gene in the PF suture may result in a more severe phenotype characterized by both the complete lack of cartilage formation and PF suture closure throughout life-time. Experiments using siRNA technique are underway to test this hypothesis. However, an alternative explanation for the presence of impaired PF suture closure, observed in *Wnt1-Cre Sox9^{flox}* older mice could be that the CNC-derived cells present in the PF suture respecify themselves into an osteoblast lineage, indeed forming patchy bony bridge within the suture.

Akiyama et al. in their study on *Wnt1-Cre Sox9^{flox}* mice showed that inactivation of *Sox9* in CNC cells resulted in a complete defect of CNC-derived endochondral bone formation, but that intramembranous bones formed normally. In addition, their experiments strongly suggested that *Sox9*-null CNC derived cells, which were blocked from differentiating into chondrocytes, expressed instead osteoblast marker genes, suggesting that *Sox9*-null CNC-derived cells were respecified into an osteoblast lineage. Therefore, at the moment we cannot rule out the possibility that the *Sox9*-null CNC-derived cells in the PF suture can be respecified into an osteoblast lineage, forming a poor bony bridge within the suture. Thus, the use of *Wnt1-Cre Sox9*, which is specific to neural crest and some parts of the brain, indicated that the cells contributing to the cartilage formation and subsequent endochondral ossification of PF suture are of neural crest origin. Furthermore, it demonstrated that *Sox9* plays an important role in PF suture closing. Therefore, we conclude that neural crest cell determinant genes such us *Sox9* regulates PF suture closure. This is to our knowledge the first report describing a specific role of a neural crest cell determinant gene in PF cranial suture patterning and closure. Our work has shown that there is a territory within the PF mesenchymal suture under control of *Sox9* gene which induces cartilage differentiation followed by endochondral ossification. This finding supports a model of autonomous endochondral ossification occurring in the skull vault where the intramembranous ossification is a major player.

Conclusions

The neural crest derived PF suture is endowed with a sophisticated architecture comprised of two layers of bone: the ectocranial and the endocranial layer. The endocranial layer of PF suture closes during the second week of life. This interesting and unique pattern of PF suture closure is characterized by a sharp and temporo-spatial up-regulated *Sox9* gene expression, and chondrogenic domains which mark precise boundaries for the areas of closure within the PF suture. We have presented evidence showing an up-regulation of *Sox9* gene expression, followed by a chondrogenesis process occurring within the PF suture during its closure. Moreover, our data demonstrated endochondral ossification as the major event leading to PF suture closure. Finally, haploinsufficiency of *Sox9* in NCC-derived cells resulted in a severe impairment of chondrogenesis as well as PF suture closure. These results strongly suggest that the unique expression of *Sox9* in the PF suture may provide inductive signal(s) for postnatal PF suture patterning and closure.

Acknowledgments

The authors wish to thank Marie-Christine Chaboissier, Andreas Schedl (INSERM U470, Centre de Biochimie, Nice, France) and Benoit de Crombrugghe (University of Texas, M.D. Anderson Cancer Center, USA), for providing

the *Sox9*/flox mice. We thank Dr. Karl Sylvester for the critical reading of the manuscript. This work was supported by NIH grants R01DE13194 and R01DE14526 and the Oak Foundation to M.T.L.

References

Akiyama, H., Chaboissier, M.C., Martin, J.F., Schedl, A., de Crombrugghe, B., 2002. The transcription factor Sox9 has essential roles in successive steps of the chondrocyte differentiation pathway and is required for expression of Sox5 and Sox6. Genes Dev. 16, 2813–2828.

Bell, D.M., Leung, K.K., Wheatley, S.C., Ng, L.J., Zhou, S., Ling, K.W., Sham, M.H., Koopman, P., Tam, P.P., Cheah, K.S., 1997. SOX9 directly regulates the type-II collagen gene. Nat. Genet. 16, 174–178.

Bellus, G.A., Gaudenz, K., Zackai, E.H., Clarke, L.A., Szabo, J., Francomano, C.A., Muenke, M., 1996. Identical mutations in three different fibroblast growth factor receptor genes in autosomal dominant craniosynostosis syndromes. Nat. Genet. 14, 174–176.

Bi, W., Huang, W., Whitworth, D.J., Deng, J.M., Zhang, Z., Behringer, R.R., de Crombrugghe, B., 2001. Haploinsufficiency of Sox9 results in defective cartilage primordia and premature skeletal mineralization. Proc. Natl. Acad. Sci. U. S. A. 98, 6698–6703.

Bradley, J.P., Levine, J.P., Roth, D.A., McCarthy, J.G., Longaker, M.T., 1996. Studies in cranial suture biology: IV. Temporal sequence of posterior frontal cranial suture fusion in the mouse. Plast. Reconstr. Surg. 98, 1039–1045.

Bronner-Fraser, M., 1994. Neural crest cell formation and migration in the developing embryo. FASEB J. 8, 699–706.

Cheung, M., Briscoe, J., 2003. Neural crest development is regulated by the transcription factor Sox9. Development 130, 5681–5693.

Couly, G.F., Coltey, P.M., Le Douarin, N.M., 1993. The triple origin of skull in higher vertebrates: a study in quail-chick chimeras. Development 117, 409–429.

de Crombrugghe, B., Lefebvre, V., Behringer, R.R., Bi, W., Murakami, S., Huang, W., 2000. Transcriptional mechanisms of chondrocyte differentiation. Matrix Biol. 19, 389–394.

Foster, J.W., Dominguez-Steglich, M.A., Guioli, S., Kowk, G., Weller, P.A., Stevanovic, M., Weissenbach, J., Mansour, S., Young, I.D., Goodfellow, P.N., et al., 1994. Campomelic dysplasia and autosomal sex reversal caused by mutations in an SRY-related gene. Nature 372, 525–530.

Gorlin, R.J., Cohen, M.J., Levin, L., 1990. Syndromes of the head and neck. Oxford University, New York.

Greenwald, J.A., Mehrara, B.J., Spector, J.A., Warren, S.M., Fagenholz, P.J., Smith, L.E., Bouletreau, P.J., Crisera, F.E., Ueno, H., Longaker, M.T., 2001. In vivo modulation of FGF biological activity alters cranial suture fate. Am. J. Pathol. 158, 441–452.

Gu, H., Marth, J.D., Orban, P.C., Mossmann, H., Rajewsky, K., 1994. Deletion of a DNA polymerase beta gene segment in T cells using cell type-specific gene targeting. Science 265, 103–106.

Haas, A.R., Tuan, R.S., 1999. Chondrogenic differentiation of murine C3H10T1/2 multipotential mesenchymal cells: II. Stimulation by bone morphogenetic protein-2 requires modulation of N-cadherin expression and function. Differentiation 64, 77–89.

Howard, T.D., Paznekas, W.A., Green, E.D., Chiang, L.C., Ma, N., Ortiz de Luna, R.I., Garcia Delgado, C., Gonzalez-Ramos, M., Kline, A.D., Jabs, E.W., 1997. Mutations in TWIST, a basic helix-loop-helix transcription factor, in Saethre–Chotzen syndrome. Nat. Genet. 15, 36–41.

Ignelzi Jr., M.A., Wang, W., Young, A.T., 2003. Fibroblast growth factors lead to increased Msx2 expression and fusion in calvarial sutures. J. Bone Miner. Res. 18, 751–759.

Iseki, S., Wilkie, A.O., Heath, J.K., Ishimaru, T., Eto, K., Morriss-Kay, G.M., 1997. Fgfr2 and osteopontin domains in the developing skull vault are mutually exclusive and can be altered by locally applied FGF2. Development 124, 3375–3384.

Ishii, M., Merrill, A.E., Chan, Y.S., Gitelman, I., Rice, D.P., Sucov, H.M., Maxson Jr., R.E., 2003. Msx2 and Twist cooperatively control the development of the neural crest-derived skeletogenic mesenchyme of the murine skull vault. Development 130, 6131–6142.

Jabs, E.W., Muller, U., Li, X., Ma, L., Luo, W., Haworth, I.S., Klisak, I., Sparkes, R., Warman, M.L., Mulliken, J.B., et al., 1993. A mutation in the homeodomain of the human MSX2 gene in a family affected with autosomal dominant craniosynostosis. Cell 75, 443–450.

Jiang, R., Lan, Y., Norton, C.R., Sundberg, J.P., Gridley, T., 1998. The Slug gene is not essential for mesoderm or neural crest development in mice. Dev. Biol. 198, 277–285.

Jiang, X., Iseki, S., Maxson, R.E., Sucov, H.M., Morriss-Kay, G.M., 2002. Tissue origins and interactions in the mammalian skull vault. Dev. Biol. 241, 106–116.

Kim, H.J., Rice, D.P., Kettunen, P.J., Thesleff, I., 1998. FGF-, BMP- and Shh-mediated signalling pathways in the regulation of cranial suture morphogenesis and calvarial bone development. Development 125, 1241–1251.

Kosher, R.A., Kulyk, W.M., Gay, S.W., 1986. Collagen gene expression during limb cartilage differentiation. J. Cell Biol. 102, 1151–1156.

LaBonne, C., Bronner-Fraser, M., 1999. Molecular mechanisms of neural crest formation. Annu. Rev. Cell Dev. Biol. 15, 81–112.

Le Douarin, N.M., Kalcheim, C., 1999. The neural crest. Cambridge Univ. Press, UK.

Le Lievre, C.S., 1978. Participation of neural crest-derived cells in the genesis of the skull in birds. J. Embryol. Exp. Morphol. 47, 17–37.

Lefebvre, V., Huang, W., Harley, V.R., Goodfellow, P.N., de Crombrugghe, B., 1997. SOX9 is a potent activator of the chondrocyte-specific enhancer of the pro alpha1(II) collagen gene. Mol. Cell. Biol. 17, 2336–2346.

Liu, Y.H., Tang, Z., Kundu, R.K., Wu, L., Luo, W., Zhu, D., Sangiorgi, F., Snead, M.L., Maxson, R.E., 1999. Msx2 gene dosage influences the number of proliferative osteogenic cells in growth centers of the developing murine skull: a possible mechanism for MSX2-mediated craniosynostosis in humans. Dev. Biol. 205, 260–274.

Manzanares, M.C., Goret-Nicaise, M., Dhem, A., 1988. Metopic sutural closure in the human skull. J. Anat. 161, 203–215.

Mayor, R., Young, R., Vargas, A., 1999. Development of neural crest in *Xenopus*. Curr. Top. Dev. Biol. 43, 85–113.

Meyers, G.A., Day, D., Goldberg, R., Daentl, D.L., Przylepa, K.A., Abrams, L.J., Graham Jr., J.M., Feingold, M., Moeschler, J.B., Rawnsley, E., Scott, A.F., Jabs, E.W., 1996. FGFR2 exon IIIa and IIIc mutations in Crouzon, Jackson-Weiss, and Pfeiffer syndromes: evidence for missense changes, insertions, and a deletion due to alternative RNA splicing. Am. J. Hum. Genet. 58, 491–498.

Mori-Akiyama, Y., Akiyama, H., Rowitch, D.H., de Crombrugghe, B., 2003. Sox9 is required for determination of the chondrogenic cell lineage in the cranial neural crest. Proc. Natl. Acad. Sci. U. S. A. 100, 9360–9365.

Morriss-Kay, G.M., 2001. Derivation of the mammalian skull vault. J. Anat. 199, 143–151.

Moss, M.L., 1958. Fusion of the frontal suture in the rat. Am. J. Anat. 102, 141–165.

Muenke, M., Schell, U., Hehr, A., Robin, N.H., Losken, H.W., Schinzel, A., Pulleyn, L.J., Rutland, P., Reardon, W., Malcolm, S., et al., 1994. A common mutation in the fibroblast growth factor receptor 1 gene in Pfeiffer syndrome. Nat. Genet. 8, 269–274.

Murakami, S., Kan, M., McKeehan, W.L., de Crombrugghe, B., 2000. Up-regulation of the chondrogenic Sox9 gene by fibroblast growth factors is mediated by the mitogen-activated protein kinase pathway. Proc. Natl. Acad. Sci. U. S. A. 97, 1113–1118.

Ng, L.J., Wheatley, S., Muscat, G.E., Conway-Campbell, J., Bowles, J., Wright, E., Bell, D.M., Tam, P.P., Cheah, K.S., Koopman, P., 1997. SOX9 binds DNA, activates transcription, and coexpresses with type II collagen during chondrogenesis in the mouse. Dev. Biol. 183, 108–121.

Nieto, M.A., Sargent, M.G., Wilkinson, D.G., Cooke, J., 1994. Control of cell behavior during vertebrate development by Slug, a zinc finger gene. Science 264, 835–839.

Noden, D.M., 1975. An analysis of migratory behavior of avian cephalic neural crest cells. Dev. Biol. 42, 106–130.

Opperman, L.A., 2000. Cranial sutures as intramembranous bone growth sites. Dev. Dyn. 219, 472–485.

Opperman, L.A., Sweeney, T.M., Redmon, J., Persing, J.A., Ogle, R.C., 1993. Tissue interactions with underlying dura mater inhibit osseous obliteration of developing cranial sutures. Dev. Dyn. 198, 312–322.

Rice, D.P., Aberg, T., Chan, Y., Tang, Z., Kettunen, P.J., Pakarinen, L., Maxson, R.E., Thesleff, I., 2000. Integration of FGF and TWIST in calvarial bone and suture development. Development 127, 1845–1855.

Rice, D.P., Rice, R., Thesleff, I., 2003. Molecular mechanisms in calvarial bone and suture development, and their relation to craniosynostosis. Eur. J. Orthod. 25, 139–148.

Roth, D.A., Bradley, J.P., Levine, J.P., McMullen, H.F., McCarthy, J.G., Longaker, M.T., 1996. Studies in cranial suture biology: part II. Role of the dura in cranial suture fusion. Plast. Reconstr. Surg. 97, 693–699.

Sarkar, S., Petiot, A., Copp, A., Ferretti, P., Thorogood, P., 2001. FGF2 promotes skeletogenic differentiation of cranial neural crest cells. Development 128, 2143–2152.

Selleck, M.A., Scherson, T.Y., Bronner-Fraser, M., 1993. Origins of neural crest cell diversity. Dev. Biol. 159, 1–11.

Sood, S., Eldadah, Z.A., Krause, W.L., McIntosh, I., Dietz, H.C., 1996. Mutation in fibrillin-1 and the Marfanoid-craniosynostosis (Shprintzen–Goldberg) syndrome. Nat. Genet. 12, 209–211.

Spokony, R.F., Aoki, Y., Saint-Germain, N., Magner-Fink, E., Saint-Jeannet, J.P., 2002. The transcription factor Sox9 is required for cranial neural crest development in *Xenopus*. Development 129, 421–432.

von der Mark, K., 1980. Immunological studies on collagen type transition in chondrogenesis. Curr. Top. Dev. Biol. 14, 199–225.

Wagner, T., Wirth, J., Meyer, J., Zabel, B., Held, M., Zimmer, J., Pasantes, J., Bricarelli, F.D., Keutel, J., Hustert, E., et al., 1994. Autosomal sex reversal and campomelic dysplasia are caused by mutations in and around the SRY-related gene SOX9. Cell 79, 1111–1120.

Warren, S.M., Brunet, L.J., Harland, R.M., Economides, A.N., Longaker, M.T., 2003. The BMP antagonist noggin regulates cranial suture fusion. Nature 422, 625–629.

Wilkie, A.O., 1997. Craniosynostosis: genes and mechanisms. Hum. Mol. Genet. 6, 1647–1656.

Wilkie, A.O., Morriss-Kay, G.M., 2001. Genetics of craniofacial development and malformation. Nat. Rev., Genet. 2, 458–468.

Wright, E., Hargrave, M.R., Christiansen, J., Cooper, L., Kun, J., Evans, T., Gangadharan, U., Greenfield, A., Koopman, P., 1995. The Sry-related gene Sox9 is expressed during chondrogenesis in mouse embryos. Nat. Genet. 9, 15–20.

Zehentner, B.K., Dony, C., Burtscher, H., 1999. The transcription factor Sox9 is involved in BMP-2 signaling. J. Bone Miner. Res. 14, 1734–1741.

Zhao, Q., Eberspaecher, H., Lefebvre, V., De Crombrugghe, B., 1997. Parallel expression of Sox9 and Col2a1 in cells undergoing chondrogenesis. Dev. Dyn. 209, 377–386.